Quasiparticle properties of graphene antidot lattices

René Petersen and Thomas Garm Pedersen*
Department of Physics and Nanotechnology, Aalborg University, DK-9220 Aalborg East, Denmark
(Received 17 February 2009; published 21 September 2009)

A periodic array of holes (antidot lattice) transforms graphene from a semimetal into a semiconductor with a tunable band gap. The magnitude of the gap is highly sensitive to the size and separation of the holes. In the present work, the properties of graphene antidot lattices are analyzed using atomistic models. Density-functional theory (DFT) and tight-binding parameterization of DFT bands usually underestimate band gaps and generally produce incorrect results for other properties related to excited states. To correct this error we consider quasiparticle (QP) corrections to the band structure of graphene antidot lattices within the tight-binding parameterization of the graphene QP band structure of Grüneis *et al.* [Phys. Rev. B **78**, 205425 (2008)]. In addition, the optical response is calculated from the QP band structure. We find that band gaps increase by about 15% in the QP model when the hole is small compared to the unit cell. Finally, QP effects on excitons are addressed using the Wannier model with a spatially varying screening.

DOI: 10.1103/PhysRevB.80.113404 PACS number(s): 73.21.−b, 78.67.−n

Graphene has recently emerged as a promising candidate for nanoscale electronics[1] with measured values of the electron mobility as high as 200 000 $cm^2\ V^{-1}\ s^{-1}$.[2,3] Such a high mobility reflecting the excellent structural quality could make ballistic transport over a range of micrometers possible and might even allow for ballistic field effect transistors (FETs).[4] However, regular graphene is a semimetal, which makes it unsuitable for usual electronic applications requiring a band gap. Hence, a variety of ways of creating semiconducting graphene have been devised. For example, by slicing it into graphene nanoribbons (GNRs),[5] a gap tunable by adjusting the GNR width can be created.[6] GNRs can be produced by relatively simple lithographic methods and usage in field effect transistors has been proposed.[7,8]

Recently, another approach to making gapped graphene has been suggested.[9] By introducing a periodic array of holes into the graphene layer a band gap, tunable by adjusting the hole size and separation, opens up at the Γ point in the Brillouin zone. To assess the feasibility and performance of these structures it is important to develop reliable models of the electronic structure. Previously, band structures and optical spectra of graphene antidot structures have been calculated in a simple tight-binding (TB) model neglecting overlap and considering only nearest neighbor (NN) interactions.[9,10] While this model reproduces the linear band structure with the correct slope (Fermi velocity) in the vicinity of the Fermi level, it should be used with care in the rest of the Brillouin zone, in particular for higher-excited states. It is by now well established that quasiparticle (QP) effects are crucial for a correct description of excited states in semiconductors.[11,12] Essentially, DFT is a theory for the ground state only and so DFT band structures typically underestimate band gaps and yield incorrect conduction band effective masses. Accordingly, TB parameterizations of DFT band structures are expected to suffer from the same deficiencies. The present work extends upon our previous work by employing the TB model of Grüneis *et al.*,[13] which incorporates QP effects by fitting the *ab initio* GW band structure of graphene in an accurate model including overlap of atomic wave functions and interactions up to third nearest neighbors. Thus, the interactions of an atom in the graphene sheet with atoms within a distance of $2a_0/\sqrt{3}$, with a_0 being the graphene lattice constant, are included in the calculations. This model is in excellent agreement with experimental data for graphite and few-layer graphene[13] and similar agreement is expected for antidot lattices. A detailed study of QP effects on band structure, band gaps and optical properties is presented. Also, the influence on two-dimensional (2D) excitons is addressed.

The antidot lattice geometries are set up according to the prescription in Ref. 9. A given structure is designated $\{L,R\}$, where $\sqrt{3}L$ and R denote the antidot lattice constant and hole radius, respectively, both in units of a_0. For planar, suspended graphene structures, σ and π electron states decouple completely, and we only solve the (generalized) eigenvalue problem for the π electron band structure. We stress that $\sigma-\pi$ decoupling is exact even in the presence of holes provided a perfectly planar geometry is maintained. Hole edges require a modification of hopping integrals, but it has been shown that such modifications only produce a minor additional opening of the gap[9] and we therefore ignore this correction. For clarity, we refer below to the simple orthogonal TB model with nearest neighbor interactions as "NN-TB" and the QP parameterization as "QP-TB." To quantify the impact of QP effects, we compare band structures, energy gaps and optical properties as predicted by the two approaches. Most importantly, we demonstrate that a simple trend for the QP correction to the band gap can be established.

We illustrate the differences between the NN-TB and QP-TB models by considering {10,3} and {17,5} antidot structures. These represent cases of medium and large structures approaching what can be fabricated experimentally.[14] The band structures of these structures calculated in the QP-TB and NN-TB models are compared in Fig. 1. Note that in both parametrizations, the Fermi level (K point) of graphite is taken as the zero point of energy. In the QP-TB model, it is seen that the band structure is no longer symmetric about the band gap. This is due to the inclusion of the overlap between atomic wave functions and interactions beyond nearest neighbors. The asymmetry has the impact that effective electron and hole masses are no longer equal. For the

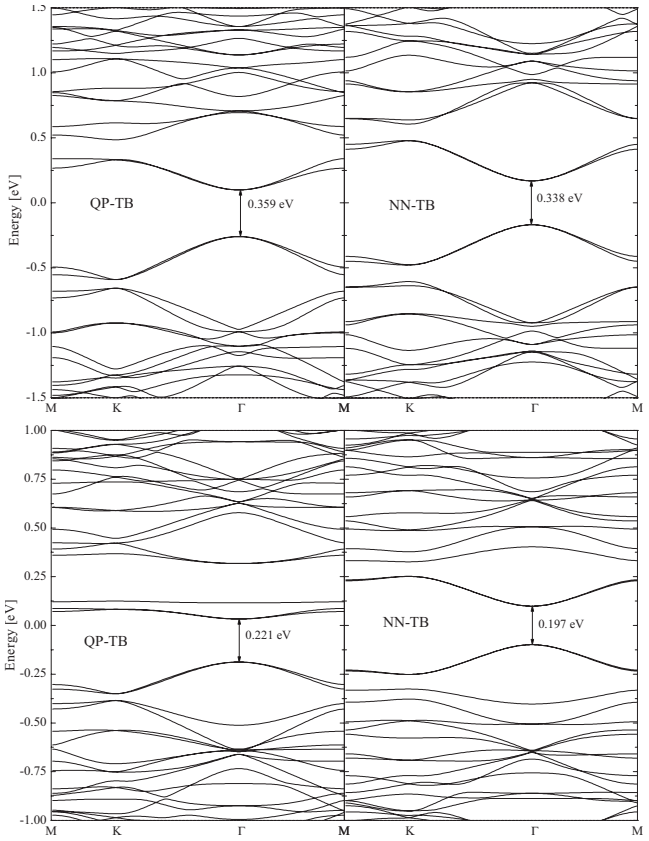

FIG. 1. The band structure of {10,3} (upper panel) and {17,5} (lower panel) antidot lattices calculated using the QP-TB model (left) and NN-TB model (right).

structures shown the band gap is increased slightly when using the QP-TB model. The NN-TB and QP-TB models agree on a vanishing band gap for regular graphene and, accordingly, the difference between predicted band gaps tends to be small for structures with a small hole compared to the size of the unit cell, i.e., whenever the hole is only a minor perturbation. The relative difference, however, may still be pronounced, as demonstrated below. In addition, other features of the band structure are subject to change even if the band gap is small. As illustrated in the lower panel of Fig. 1, the asymmetry of valence and conduction bands of a {17,5} antidot lattice is obvious and overall the band structure undergoes quite a change from the NN-TB to the QP-TB model. Generally, in the QP-TB model the conduction bands are compressed. Also, the lowest group of conduction bands tend to form an isolated band with rather low curvature, i.e., large effective electron masses. As a result, electron mobilities are expected to be sensitive to QP effects.

To quantify the trend in the band gap corrections we have considered a wide range of structures defined by the total number of carbon atoms in a unit cell before any perforation is made N_{total} and the number of atoms removed to form the hole N_{removed}.[9] If the band gap is plotted versus $N_{\text{removed}}^{1/2}/N_{\text{total}}$ for various antidot structures a roughly linear behavior is observed for both the NN-TB and QP-TB model as can be seen in Fig. 2. The effect of QP corrections raises the band gap about 15% above the NN band gap when the ratio of

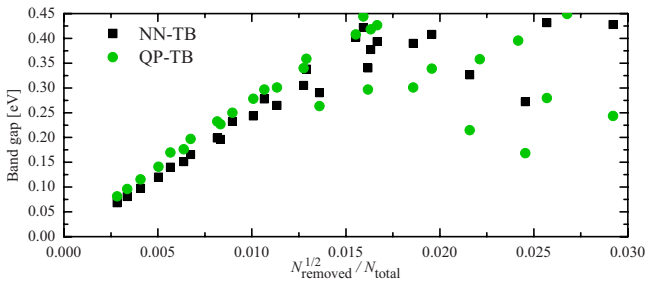

FIG. 2. (Color online) Plot of the band gap vs $N_{\text{removed}}^{1/2}/N_{\text{total}}$ for various antidot structures. The QP-TB band gaps generally lie higher than the NN-TB gaps when the ratio is small.

removed to total number of atoms is small. It should be pointed out that realistic structures generally lie in the left part of the plot since large holes in small unit cells could cause crumbling of the graphene sheet. Hence, the present work shows that QP corrections are indeed important for realistic graphene antidot lattices. Moreover, the predicted increase of the band gap makes such structures even more attractive for device applications. We emphasize that the increased band gap is not a consequence of an increased slope of the linear part of the graphene band structure. In fact, both models predict similar Fermi velocities of around 9.9×10^5 m/s.

Numerically, the QP-TB model predicts a band gap that can be closely fitted as $E_g = 29\ \text{eV} \cdot N_{\text{removed}}^{1/2}/N_{\text{total}}$ in the limit $N_{\text{removed}}^{1/2}/N_{\text{total}} \ll 1$, cf. Figure 2. At present, no experimental data exist for the small structures that can be described theoretically. Recently, however, Eroms and Weiss[15] have fabricated square antidot lattices with lattice constants of 90 nm and hole diameters of approximately 60 nm. Hence, the present gap formula would predict an energy gap of 30 meV, clearly larger than the value of 6 meV deduced from experimental I/V curves.[15] The uncertainty on the experimental gap is not known and may account for part of the discrepancy. Moreover, the experimental samples differ from the idealized ones considered here. Finally, it is conceivable that differences in lattice geometry (square vs hexagonal) are important.

With the band structure available the calculation of the absorption spectra is straightforward. The point we wish to address is the following: will QP corrections simply rigidly shift the spectra to higher energies, similarly to the case of most inorganic semiconductors,[11,12] or do more substantial changes follow from redistribution of oscillator strength? Following Ref. 10, we calculate here the real part of the conductivity $\sigma(\omega)$, which corresponds to the absorption. The same triangle integration method as the one used in[10] is applied and 4096 triangles are used. In Fig. 3, the spectra of antidot lattices {12,1}, {12,3}, {12,4.2}, and {12,5} are shown ($R=4.0$ is avoided because it leads to unphysical geometries). Only the ideal case of vanishing broadening and doping is considered. The conductivity is given in units of the low-frequency optical conductivity of regular graphene $\sigma_0 = e^2/4\hbar$.[9,15] The dash-dotted curves are calculated in the NN-TB model and the solid curves in the QP-TB model. These spectra support the aforementioned point that the band gap increases in QP-TB due to the QP effects when the ratio

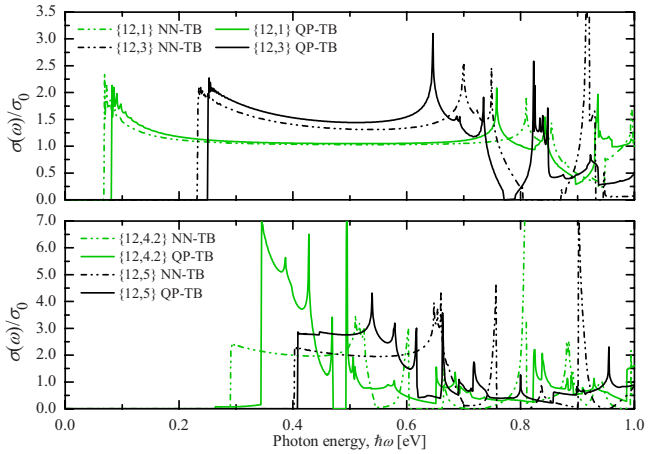

FIG. 3. (Color online) Conductivity spectra σ/σ_0 of {12,1}, {12,3}, {12,4.2}, and {12,5} antidot lattices calculated in both the NN-TB (dash-dotted) and QP-TB (solid) TB model.

$N_{\text{removed}}/N_{\text{total}}$ is small, i.e., for {12,1} and {12,3}. For larger ratios, {12,4.2} and {12,5}, quite drastic changes are observed and the band gap actually decreases in the QP-TB model. For the {12,4.2} structure the QP-TB band gap (0.26 eV) lies below the NN-TB gap but the absorption there is very low. This is because the ordering of the lowest-conduction bands at Γ differs: in the NN-TB model, the lowest band is twofold degenerate and the second lowest is nondegenerate, while the order is reversed in the QP-TB model. This results in one band with a low-transition probability (0.26 eV absorption edge) and one with a high-transition probability (0.34 eV absorption edge). In addition, the NN-TB spectra all conform to the rule $\sigma(\omega)/\sigma_0 \approx 2$ at the absorption edge, which follows exactly from a continuum approximation for gapped graphene.[16] In the QP-TB case, however, this rule is strongly disobeyed for large-hole cases. This substantial shift of oscillator strength shows that QP corrections in optical spectra cannot generally be approximated by rigidly shifting the conduction bands, i.e., applying the "scissors operator."

In the calculation of the optical spectra, excitonic effects have not been included. A rigorous description of excitonic effects in the present structures is a difficult task but the Wannier model can be used as a good starting point.[17] In previous work,[16] we estimated exciton effects for graphene on SiO_2 by considering screening by the substrate only. Here, we wish to improve this estimate by (i) employing more accurate QP-TB effective masses, and (ii) incorporating screening by the graphene layer itself. The pronounced nonlocality of screening in gapped graphene means that a spatially varying dielectric constant (the dielectric function) $\varepsilon(r)$ must be allowed for.[18] Hence, we solve the Wannier equation $[-\nabla^2 - 2/(r\varepsilon(r))]\varphi(\boldsymbol{r}) = E\varphi(\boldsymbol{r})$, where r is measured in units of the effective (unscreened) Bohr radius $a_0^* = 0.529\ \text{Å} \cdot m_0/\mu$ with m_0 the free electron mass and $\mu = m_e m_h/(m_e + m_h)$ the reduced electron-hole pair mass and where the energy is measured in effective Rydbergs $Ry^* = \hbar^2/(2\mu a_0^{*2})$. We calculate $\varepsilon(r)$ from the procedure described by Pyatkovskiy[18] for vanishing chemical potential. In the Dirac model of gapped graphene, the energy dispersion is approximated as $E_{c/v,\boldsymbol{k}} = \pm\sqrt{\alpha^2 + \hbar^2 v_F^2 k^2}$, where $2\alpha = E_g$ and

TABLE I. Excitonic binding energies E_B along with band gap E_g and effective electron and hole masses for a few structures.

	{10,1}	{10,3}	{12,1}	{12,3}
E_B [meV]	−25	−94	−17	−62
E_g [meV]	115	358	81	250
m_e [m_0]	0.012	0.053	0.008	0.033
m_h [m_0]	0.012	0.047	0.008	0.031

v_F is the graphene Fermi velocity. Here, k is measured relative to the Γ point rather than the K point since the band extrema are located at Γ as can be seen from Fig. 1. It follows from the polarization function Π of Ref. 18 that the static 2D sheet susceptibility $\chi_{2D} \propto \Pi/q$ in 2D momentum q space has the asymptotic behaviors

$$\chi_{2D}(q) = \begin{cases} \dfrac{e^2}{8\varepsilon_0 \hbar v_F} \equiv \kappa, & q \to \infty \\ \dfrac{4\kappa}{3\pi} \cdot \dfrac{\hbar v_F q}{\alpha}, & q \to 0 \end{cases}. \tag{1}$$

From the limiting behavior of the susceptibility an approximate expression for the effective dielectric function, which has the correct limiting behavior, can be constructed as

$$\frac{1}{\varepsilon_{\text{eff}}(q)} \approx \frac{1}{\bar{\varepsilon} + \kappa} + \frac{\kappa}{\bar{\varepsilon}(\bar{\varepsilon} + \kappa)} e^{-\beta q}, \tag{2}$$

where $\bar{\varepsilon} = (\varepsilon_{SiO_2} + \varepsilon_{\text{air}})/2 \approx 2.5$ is the average dielectric constant of substrate and air and $\beta = 4(\bar{\varepsilon} + \kappa)\hbar v_F/(3\pi\bar{\varepsilon}\alpha)$. From this expression the screened Coulomb potential in the graphene layer is found to be

$$U(r) \approx \frac{1}{(\bar{\varepsilon} + \kappa) r} + \frac{\kappa}{\bar{\varepsilon}(\bar{\varepsilon} + \kappa)\sqrt{r^2 + \beta^2}} \tag{3}$$

and writing $U(r) = 1/[r\varepsilon(r)]$ defines the dielectric function. A variational estimate of the exciton binding energy can then be obtained by writing the radial part of the 1s exciton state as $\varphi(r) = 2\eta e^{-\eta r}$. This gives the following expectation value of the exciton binding energy

$$E_B = \eta^2 - \frac{4\eta}{\bar{\varepsilon}(\bar{\varepsilon} + \kappa)} + \frac{4\pi\kappa\beta\eta^2}{\bar{\varepsilon}(\bar{\varepsilon} + \kappa)}[Y_1(2\beta\eta) + \text{H}_{-1}(2\beta\eta)], \tag{4}$$

where Y and H are Bessel and Struve functions, respectively. Here, β should be measured in units of effective Bohr radii a_0^*. Using the effective electron and hole masses determined from the curvature of the lowest conduction band and the highest-valence band in the Γ point, respectively, the value of β/a_0^* can be calculated and the optimal value of η can be determined numerically. The exciton binding energies are listed in Table I along with the effective masses and band gaps for a number of antidot lattices, all calculated in the QP-TB model. The magnitude of the excitonic energies confirms that, indeed, exciton effects are of importance in graphene antidot lattices. Typically, the binding energy is

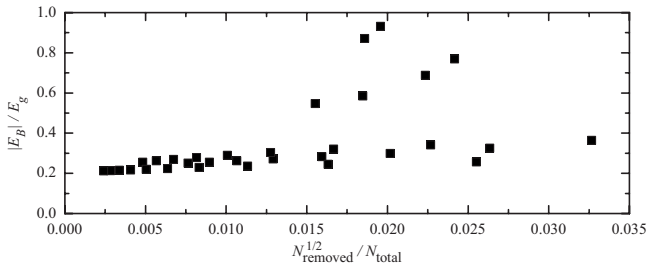

FIG. 4. The exciton-binding energy divided by the gap size plotted versus $N^{1/2}_{\mathrm{removed}}/N_{\mathrm{total}}$.

about 25% of the band gap as illustrated in Fig. 4 for a wide range of antidot lattices with physically reasonable geometries, i.e., $L>2R$. The relatively large structures that may be within experimental reach correspond to small values of $N^{1/2}_{\mathrm{removed}}/N_{\mathrm{total}}$ for which the asymptotic binding energy is approximately 20% of the gap. Compared to our previous estimate,[16] the present work shows that QP effects on the effective masses and screening by graphene itself reduces the binding energy by a factor of nearly two.

In this work, the effects of quasiparticle corrections on the electronic and optical properties of graphene antidot lattices have been analyzed. For structures having small holes compared to the lattice constant, it is demonstrated that the band gap increases by about 15% due to QP effects. These corrections are important and promising for devices relying on antidots as a means of turning graphene semiconducting. In addition, QP effects have important consequences for the optical response, leading to increased transparency windows. For large holes the optical spectra are severely modified. Thus, incorporating QP effects is essential for calculation of properties of antidot lattices involving excitations. Using the band structures from the QP model to determine effective masses, excitonic effects have been considered within a Wannier model including nonlocal screening. Our estimate for the exciton-binding energy indicates that these effects are highly important for the optical response.

ACKNOWLEDGMENTS

Financial support from the Danish FTP Research council grant "Nanoengineered graphene devices" is gratefully acknowledged.

*tgp@nano.aau.dk

[1] K. S. Novoselov, A. K. Geim, S. V. Morozov, D. Jiang, Y. Zhang, S. V. Dubonos, I. V. Grigorieva, and A. A. Firsov, Science **306**, 666 (2004).
[2] X. Du, I. Skachko, A. Barker, and E. Y. Andrei, Nat. Nanotechnol. **3**, 491 (2008).
[3] K. I. Bolotin, K. J. Sikes, J. Hone, H. L. Stormer, and P. Kim, Phys. Rev. Lett. **101**, 096802 (2008).
[4] M. I. Katsnelson, Mater. Today **10**, 20 (2007).
[5] V. Barone, O. Hod, and G. E. Scuseria, Nano Lett. **6**, 2748 (2006).
[6] M. Y. Han, B. Özyilmaz, Y. Zhang, and P. Kim, Phys. Rev. Lett. **98**, 206805 (2007).
[7] Q. Zhang, T. Fang, H. Xing, A. Seabaugh, and D. Jena, IEEE Electron Device Lett. **29**, 1344 (2008).
[8] Z. Chen, Y.-M. Lin, M. J. Rooks, and P. Avouris, Physica E (Amsterdam) **40**, 228 (2007).
[9] T. G. Pedersen, C. Flindt, J. Pedersen, N. A. Mortensen, A.-P. Jauho, and K. Pedersen, Phys. Rev. Lett. **100**, 136804 (2008).
[10] T. G. Pedersen, C. Flindt, J. Pedersen, A. P. Jauho, N. A. Mortensen, and K. Pedersen, Phys. Rev. B **77**, 245431 (2008).
[11] M. Rohlfing, P. Krüger, and J. Pollmann, Phys. Rev. B **48**, 17791 (1993).
[12] G. Onida, L. Reining, and A. Rubio, Rev. Mod. Phys. **74**, 601 (2002).
[13] A. Grüneis, C. Attaccalite, L. Wirtz, H. Shiozawa, R. Saito, T. Pichler, and A. Rubio, Phys. Rev. B **78**, 205425 (2008).
[14] M. D. Fischbein and M. Drndic, Appl. Phys. Lett. **93**, 113107 (2008).
[15] J. Eroms and D. Weiss, arXiv:0901.0840 (unpublished).
[16] T. G. Pedersen, A.-P. Jauho, and K. Pedersen, Phys. Rev. B **79**, 113406 (2009).
[17] H. Haug and S. W. Koch, *Quantum Theory of the Optical and Electronic Properties of Semiconductors* (World Scientific, Singapore, 2005).
[18] P. K. Pyatkovskiy, J. Phys.: Condens Matter **21**, 025506 (2009).